

See discussions, stats, and author profiles for this publication at:
<https://www.researchgate.net/publication/232385150>

Electronegativity and chemical hardness: Two helpful concepts for understanding oxide nanochemistry

ARTICLE *in* MATERIALS LETTERS · DECEMBER 2001

Impact Factor: 2.49 · DOI: 10.1016/S0167-577X(01)00328-7

CITATIONS

8

READS

49

7 AUTHORS, INCLUDING:



Marie Helene DELVILLE

French National Centre for Scientific R...

130 PUBLICATIONS 1,389 CITATIONS

SEE PROFILE



Mona Tréguer

French National Centre for Scientific R...

78 PUBLICATIONS 1,429 CITATIONS

SEE PROFILE



Electronegativity and chemical hardness: two helpful concepts for understanding oxide nanochemistry

C.-W. Kwon, A. Poquet, S. Mornet, G. Campet, M.-H. Delville, M. Treguer,
J. Portier *

ICMCB, UPR-CNRS 9048, 87 Avenue Dr. A. Schweitzer, 33608 Pessac Cedex, France

Received 24 January 2001; received in revised form 2 March 2001; accepted 9 March 2001

Abstract

Electronegativity, χ , as defined by Mulliken and chemical hardness, η , as proposed by Pearson are used as fundamental tools for the preparation of oxide nanoparticles and for the interpretation of their physical and chemical properties. The evolution of electronegativity and chemical hardness from crystal to nanoparticles is studied. The formation of solid particles from inorganic salt solutions is described on the basis of a χ, η plot. The correlation between the point of zero zeta potential (PZZP) and pH is studied. A model approach concerning the surface modification of oxide nanoparticles by silanization is proposed. © 2001 Elsevier Science B.V. All rights reserved.

Keywords: Electronegativity; Chemical hardness; Oxide nanoparticles

1. Introduction

The emerging field of nanotechnology is innovating many areas of chemistry, physics and technology. Quantum dots, nanoclusters, nanoparticles, nanotubes, thin films, nanoporous materials, nanowires, hybrid nanocomposites, etc., can be fashioned. They are used in numerous applications such as: catalysis, electronics, separation technologies, sensors, information storage, drug delivery systems, diagnostics (MRI), and energy (batteries, fuel cells, solar cells, ...).

The first step in nanotechnology is obviously nanochemistry, which permits to control chemical parameters in order to grow nanoobjects. In the case of oxides prepared from an aqueous solution, a

simplified and schematic process is shown in Fig. 1. A solution of a salt is treated by various chemical operations: addition of an acid or base to vary the pH, addition of molecules, etc. in order to produce a sol (step I). Oxides, hydroxides or oxyhydroxides can constitute this sol. If the compound formed is an oxide, the nanoparticles are coated following step IV. In step II, the micellar suspension is dried in order to get a gel. A second drying of the gel (step III) leads to a xerogel or aerogel that is pulverized and put in suspension in a liquid. Then, the nanoparticles can be coated, generally with molecular or polymeric species (step IV).

Indeed, such nanoparticles used in various domains and particularly in biology and medicine have to be coated with organic species (including polymers) in order to be stabilized in the utilization medium (for example, blood in medicine), and to be functionalized (cell targeting).

* Corresponding author.

E-mail address: portier@icmcb.u-bordeaux.fr (J. Portier).

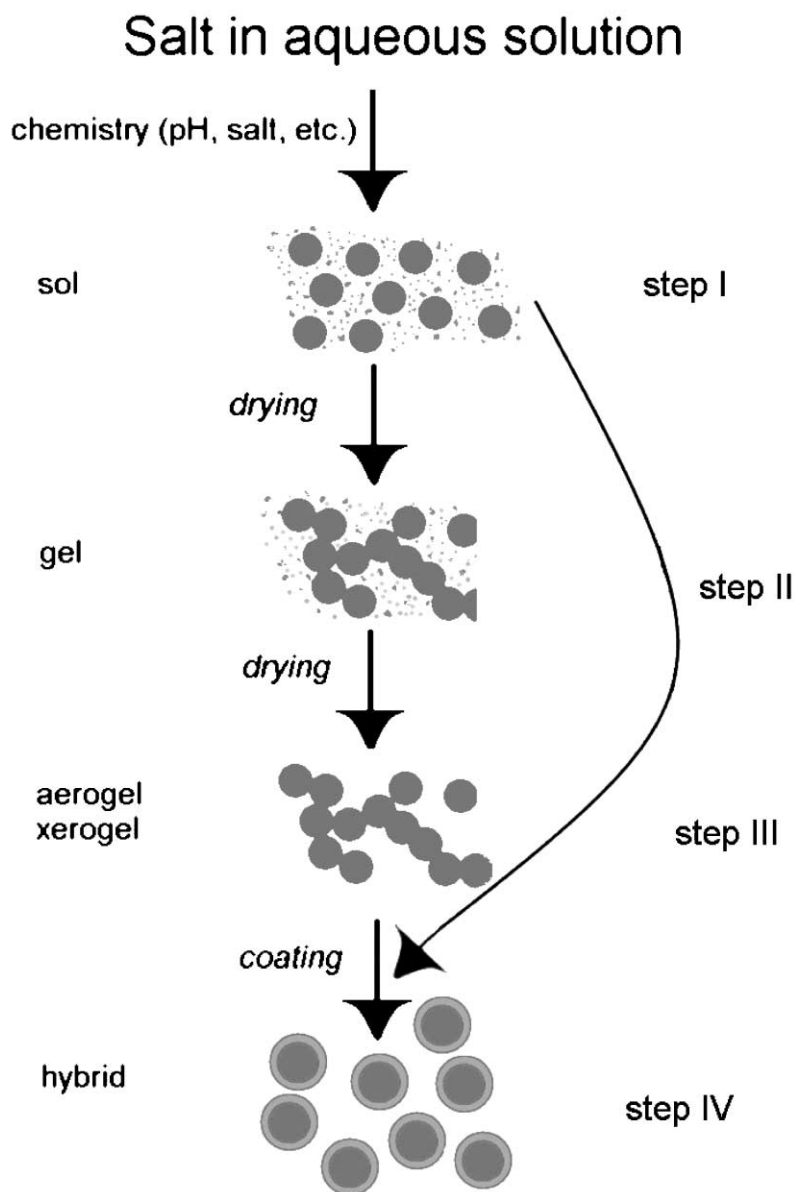


Fig. 1. Schematic chemical process used for the preparation of oxide nanoparticles.

The previous process raises several questions:

- during step I, what is the nature of the solid formed?
- is the sol stable or do the nanoparticles precipitate?
- is it possible to establish covalent bonding between the inorganic nanoparticles and the organic species used for the coating?

In this paper, we propose fundamental answers to these three questions on the basis of the electronega-

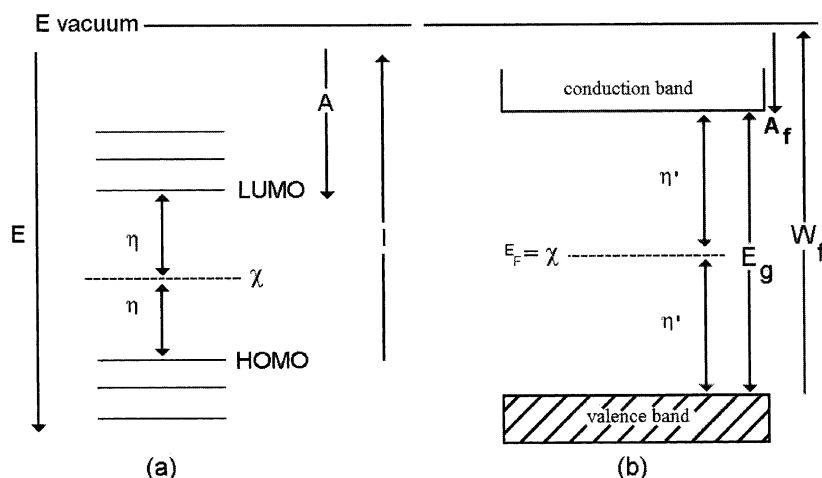


Fig. 2. Schematic energy level diagram for (a) a molecule or an ion and (b) for an arbitrary undoped semiconducting oxide showing parameters discussed in the text.

tivity χ and of the chemical hardness η of the cations and of the corresponding oxides. Indeed, χ and η determine the behaviour of a given ion in solution and, therefore, the properties of the particles coming out of this solution. These parameters play an important role in aqueous soft chemistry processes where spontaneous reactions are used to produce sols, gels, and nanoparticles.

We also discuss the evolution of χ and η from crystal to nanoparticles and show how the structural disorder affects these two parameters, leading to new specific properties.

2. Electronegativity and chemical hardness

The electronegativity concept, proposed by Pauling in 1932 [1] as “the power of an atom in a molecule to attract electrons”, is undoubtedly the

intuitive idea most widely used by chemists. Few years later, Mulliken provided a physical support to electronegativity [2]; it is the average between the absolute values of the ionisation potential I and of the electron affinity A (Fig. 2a): $\chi = 0.5(I + A)$. In 1963, Pearson proposed the concept of chemical hardness [3–5]. The empirical statement based on the observation is that “hard Lewis acids prefer to coordinate to hard Lewis bases and soft acids to soft bases”. The physical meaning of this concept has been proposed by Parr and Pearson [6]. In a molecule, the chemical hardness η is equal to $0.5(I - A)$, i.e. half the gap between the HOMO and the LUMO (Fig. 2a).

These two concepts, treated as quantum chemical parameters, can be applied to a solid (Fig. 2b). In an undoped semiconductor, having no subband-gap states, the electronegativity χ corresponds to the Fermi energy E_F and the chemical hardness η' to $0.5E_g$.

Table 1

Formula used for the various calculations (z = cationic formal charge, r = ionic radius (\AA), χ = electronegativity, η = chemical hardness, $P = z/r^2$, P.u. Pauling unit)

Cationic electronegativity	χ_{cation} (P.u.)	$\approx 0.274z - 0.15zr - 0.01r + 1 + \alpha$
Absolute cationic electronegativity	χ_{cation} (eV)	$\approx (\chi_{\text{cation}}(\text{P.u.}) + 0.206)/0.336$
Absolute oxide electronegativity	χ_{oxide} (eV)	$\approx 0.45\chi_{\text{cation}} \neq (\text{eV}) + 3.36$
Cationic acid strength	ICP (dimensionless)	$\approx \log_{10}(P) - 1.38\chi_{\text{cation}}(\text{P.u.}) + 2.07$
Chemical hardness	η' (eV)	$\approx 4.25\text{ICP} - 0.67$

In previous works, we proposed new scales for electronegativity and chemical hardness of inorganic cations [7–9] (Table 1). In this study, we will use 2D plots with χ and η as Cartesian coordinates. Indeed, an ion or an oxide is energetically and, as a result, chemically, characterized by these two parameters.

3. From crystal to nanoparticles: evolution of electronegativity and chemical hardness

In order to understand the evolution of χ and η from crystal to nanoparticles, one should first recall that a polycrystalline material is composed of grains, and that each grain can be likened to a well defined periodic array of atoms that is surrounded by a more or less disordered layer having weakened bonds and dangling bonds. When the size of the crystallites is large enough, as it occurs in Fig. 3a, the influence of the surface forces are negligible and the crystallites show their expected crystalline shape.

On the other hand, when the size of the crystallites diminishes well below 10 nm, as it occurs in Fig. 3b, the crystallites tend to loose their expected shape and to adopt that of a more pseudo spherical shape due to the natural tendency towards the minimization of the surface energy. This behaviour tends to favour the formation, at the grain surface, of: (i) weakened bonds that are associated with a reduced symmetry; (ii) dangling bonds such as anions adjacent to cation vacancies or cation adjacent to anion vacancies. This even affects somehow the periodic array in the shell of the crystallite and then, for small enough grains, the overall electronic structure is modified.

Several models have been proposed to justify the modification of the electronic structure when the periodic array is disturbed [10]. Most of them consider that the salient features of well crystallized semiconductors, i.e. the existence of sharp edges at the valence and conduction bands leading to a well defined band-energy gap, are noticeably changed when the long range and the short range orders (i.e. a few coordination spheres) are no longer preserved.

We have used these models as the basis of the following concept: it consists in illustrating the disorder in the layer at the grain surface of the nanocrystalline semiconductors by introducing sub-band-gap energy states [11–13]. These states account for the existence of:

- a band tailing near the band edges and resulting from the above mentioned bond weakening,
- deeper states which originate from the above mentioned dangling bonds.

This is illustrated in Fig. 4 for undoped and n-doped TiO_2 using, for the sake of clarity, a simplified energy diagram. TiO_2 is taken as an illustrative, but unrestricted, example [13]. In the figures, $[\text{Ti}^{4+}:3d]_{\text{subband-gap st.}}$ and $[\text{O}^{2-}:2p]_{\text{subband-gap st.}}$ represents the subband-gap energy states that include the band tailing, on the one hand, and the deeper states arising from the cation (anion) defects adjacent to anion (cation) vacancies, on the other hand.

For stoichiometric and undoped TiO_2 (Fig. 4(1)), the decrease of the size of the crystallites does not modify χ significantly at the grain surface, since E_F remains pinned near the gap center. On the contrary, the subband-gap energy states cause a decrease of

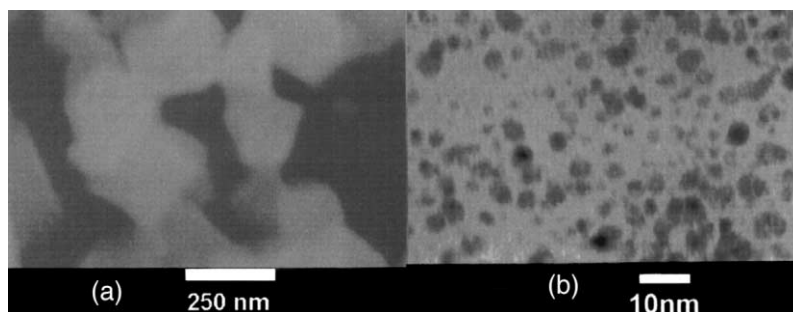


Fig. 3. Transmission electron microscopy of magnetite: (a) 250 nm crystals, (b) 5–10 nm nanocrystals.

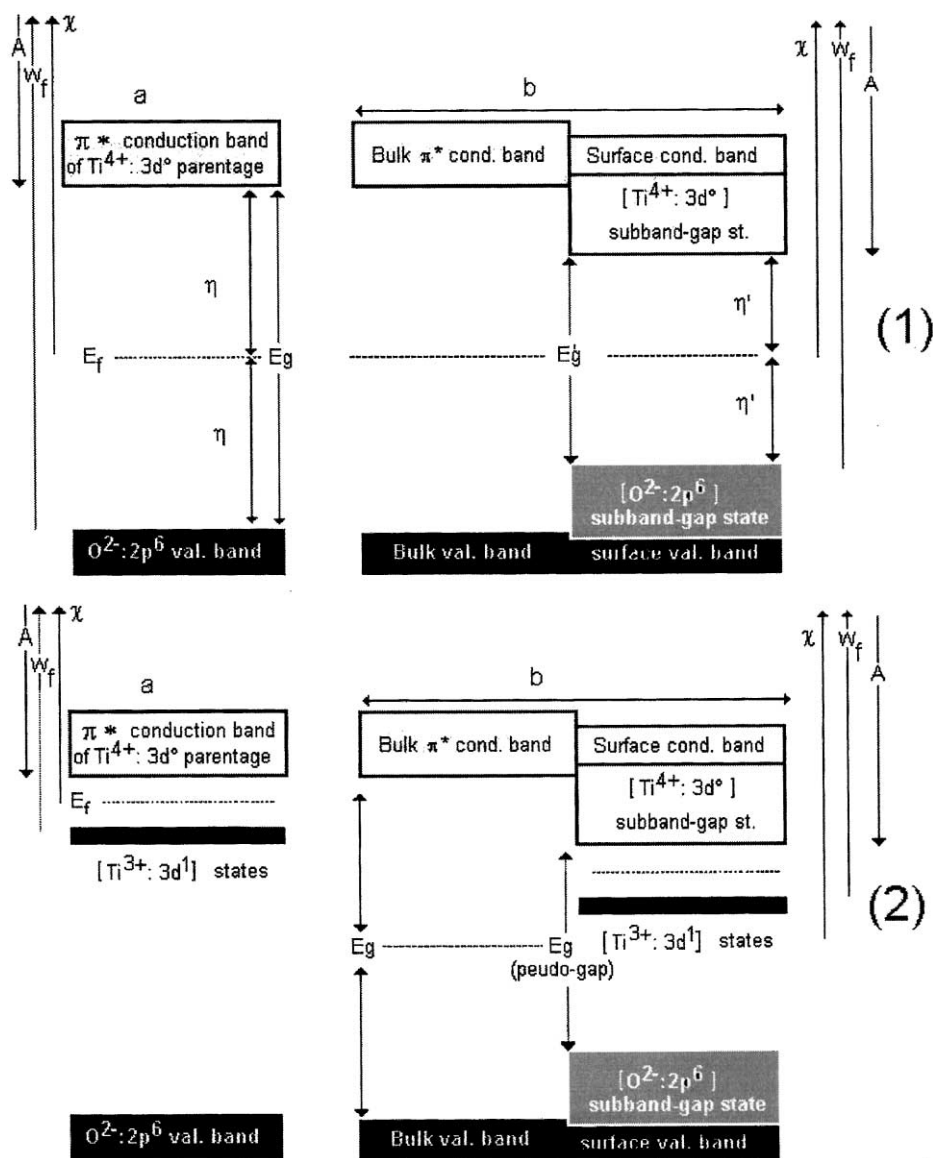


Fig. 4. Modification of the band structure, related to "surface effect", from (a) well crystallized microcrystalline to (b) poorly crystallized nanocrystalline, in (1) stoichiometric, and (2) n-type conducting TiO_2 .

the work function, W_F , and an increase of the electron affinity (absolute value), A . Consequently the chemical hardness, η , is diminished at the grain surface.

For n-type doped TiO_2 (Fig. 4(2)), the decrease in size of the crystallites induces an increase of the extrinsic work function at the grain surface since the $\text{Ti}^{3+}; 3d^1$ energy states are shifted downwards below

the $[\text{Ti}^{4+}; 3d^0]$ subband-gap energy states, which themselves are responsible for the increase of the extrinsic electron affinity (absolute value). Consequently, the extrinsic electronegativity χ is enhanced at the grain surface.

Obviously, the above observations can be easily extended to other similar semiconducting oxides, either undoped or doped. Related to that, let us quote

that, if for n-type semiconducting oxides, the surface (extrinsic) electronegativity is enhanced by the struc-

tural disorder, χ is, conversely, decreased for p-type semiconductors.

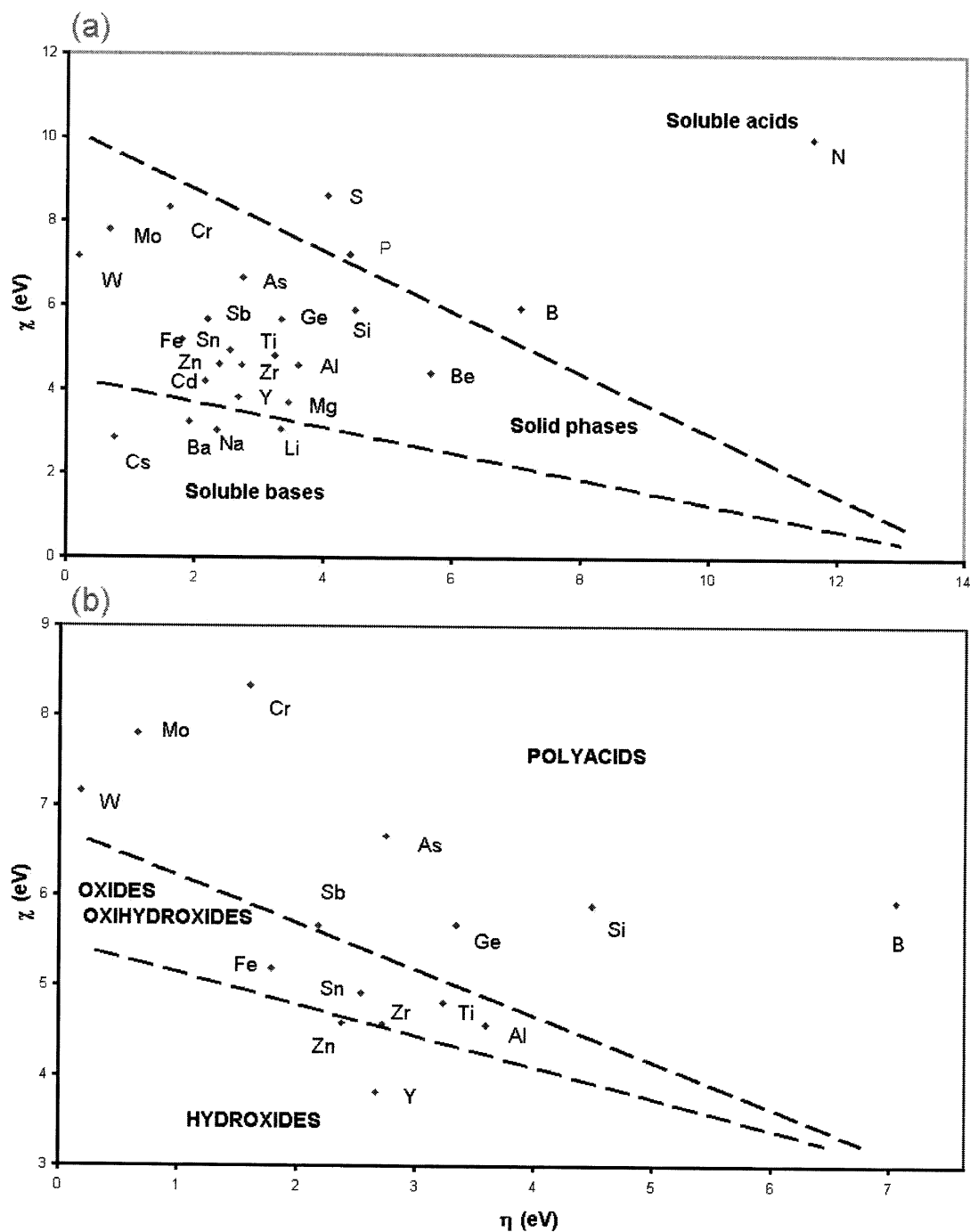


Fig. 5. χ, η plot for some cations in solution: (a) large scale, (b) zoom. χ and η have been calculated using the data in Tables 1 and 2.

Most interestingly, the above reported evolution of the intrinsic or extrinsic parameters χ , η , A , W_F , as the crystallite size decreases, accounts for the change of specific properties. For instance, the chemical and electrochemical activity of the grain surface can be strongly enhanced when its size diminishes down to the nanoscale level [13]. The increase of the chemical activity is, obviously, correlated with the decrease of the chemical hardness.

As an example, we have observed an increase of the electrochemical activity of n-type or p-type nanoscale electrodes compared to that of microcrystalline ones; this change can be correlated with an increase (n-type) or an decrease (p-type) of the extrinsic electronegativity at the grain surface. We have shown, indeed, that the grain surface of nanocrystalline n-type electrodes are often particularly suited for allowing an efficient electrochemical grafting of the cationic species (such as Li^+) issued from the electrolyte [14,15]. It necessarily means that the surface layer can be more easily reduced when the grain size decreases and this can be easily understood if the surface electronegativity has increased. Poizot et al. have recently illustrated this interpretation in studying the electrochemical behavior of nanoparticles of transition metal oxides [16].

4. Cations in aqueous solution

In step I of Fig. 1, a solution of a salt is prepared. Then, pH, concentration, temperature, etc. are varied in order to form a micellar solid. It is interesting to forecast the chemical phenomena that will occur during this process.

In the χ, η plot (Fig. 5a, Table 2), three domains clearly appear. Ions having at the same time a high electronegativity and chemical hardness have the tendency to form oxoanions leading to soluble acids. It is the case of N^{5+} , P^{5+} and S^{6+} ; HNO_3 , H_3PO_4 and H_2SO_4 acids are formed. On the contrary, the ions that simultaneously exhibit a low electronegativity and a weak chemical hardness generally form soluble bases; it is the case of alkali ions. The Pearson HSAB model explains these two behaviours: hard cations connect with the strongest base, i.e. O^{2-} anions, whereas soft cations combine with the softest base, i.e. OH^- group.

Table 2
Numerical data used in Fig. 5

Element	z	CN	χ (eV)	η (eV)	Element	z	CN	χ (eV)	η (eV)
N	5	3	10.0	2.47	Ti	4	6	4.81	3.23
S	6	4	8.63	4.06	Zn	2	4	4.59	2.8
Cr	6	4	8.33	1.60	Zr	4	7	4.57	2.73
Mo	6	4	7.80	0.66	Al	3	6	4.57	3.60
P	5	4	7.23	4.41	Be	2	4	4.41	5.67
W	6	6	7.16	0.18	Cd	2	4	4.20	2.15
As	5	4	6.66	2.75	Y	3	8	3.82	2.67
Si	4	4	5.89	4.49	Mg	2	6	3.69	3.46
Ge	4	4	5.68	3.34	Ba	2	8	3.24	1.91
Sb	5	6	5.67	2.19	Li	1	6	3.06	3.34
Fe	3	6	5.19	1.79	Na	1	6	3.03	2.33
Sn	4	6	4.92	2.54	Cs	1	8	2.86	0.75

In the intermediate domain (Fig. 5b), solid nanoparticles can be formed. Depending on the coordinates in the χ, η plot, the cations will tend to form:

- hydroxides, generally insoluble or weakly soluble (alkaline-earth cations, Pb^{2+} , rare-earth cations, etc.) near the base border
- polyacids near the acid limit
- in between, oxides or oxyhydroxides.

This behaviour is also simply explained with the HSAB principle: in this category, the cations with a moderate acid strength combine with OH^- group while those with a slightly higher acid strength forms oxyhydroxides.

This simple classification is in good agreement with that proposed by Henry et al. [17] based on a charge electronegativity diagram.

5. Nanoparticles in electrolyte

Nanoparticles in suspension in a liquid are not stable. In order to minimize the surface forces, the size of the particle tends to increase by aggregation and to precipitate due to gravity forces. This tendency to agglomerate is even stronger in case of magnetic particles (magnetite, maghemite) because of magnetic attraction of particles in presence of an external magnetic field.

Nevertheless, stable sols can be obtained. Indeed, in an electrolyte like water, the nanoparticles constitute their Helmholtz double layer described by the diffuse double layer model by attracting the negative or positive ions that are present in the electrolyte; therefore, these repulsive electric charges prevent the aggregation of particles. Fig. 6 and Table 3 illustrate this behaviour for maghemite nanoparticles in water. Stable sols are obtained in acid or basic pH domains.

Precipitation occurs when the surface charges have been neutralized (PZZP = 7.5; PZZP is the pH at which the surface charge and therefore the zeta potential is zero).

Another simple experiment illustrates this behaviour. When dry particles are continuously added to water, a variation of pH is observed. This is due to the fixation of proton or hydroxyl group in the first Helmholtz layer of the particle. After adding a given

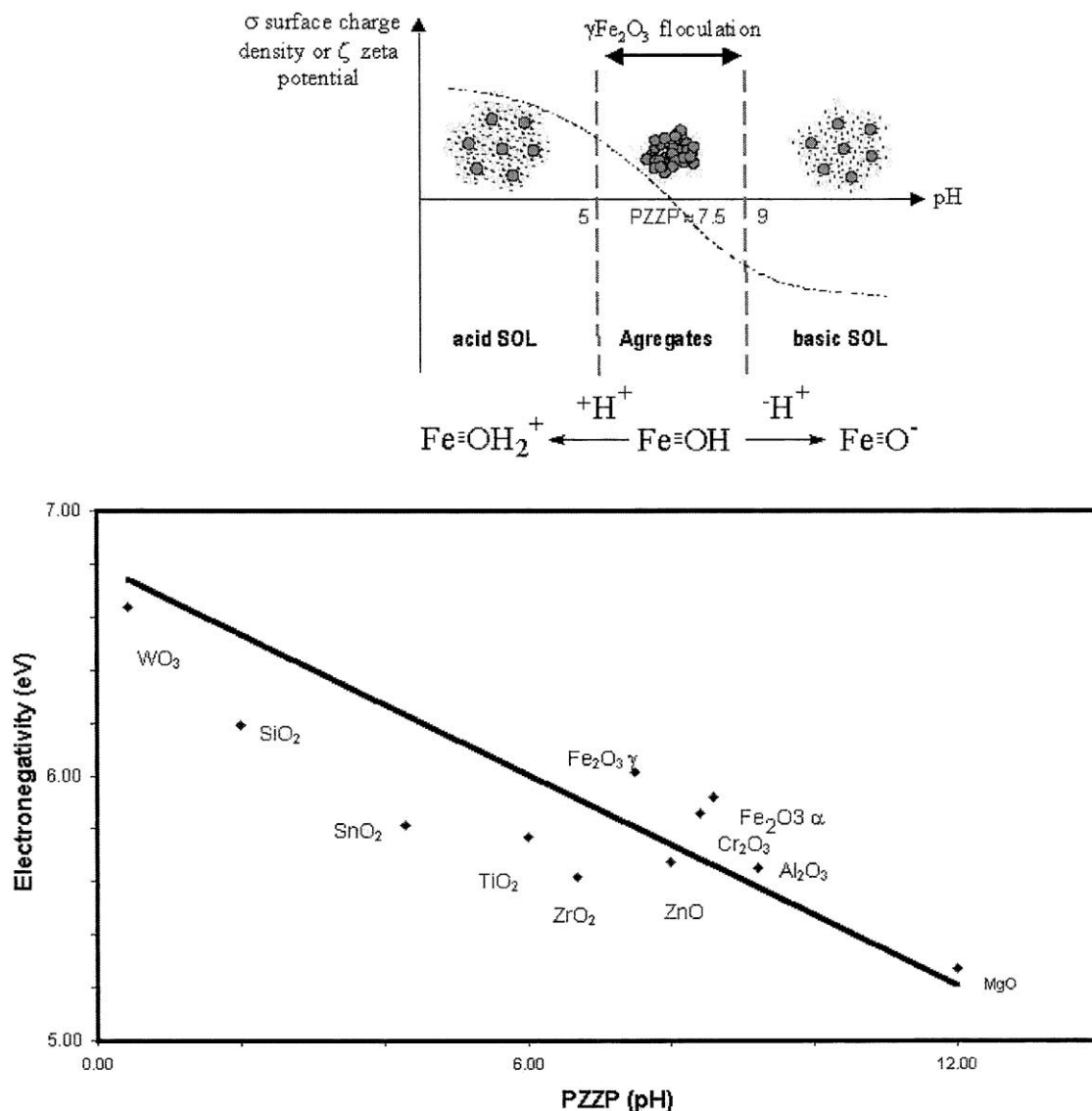


Fig. 6. Stability domain of maghemite sol and plot of the PZZP vs. calculated electronegativity of some oxides.

Table 3
Numerical data used in Fig. 6

Oxide	PZZP [11]	χ_{oxide} (eV) [this work]	χ_{oxide} (eV) [11]
MgO	12.00	5.28	5.27
ZrO ₂	6.70	5.62	5.92
Al ₂ O ₃	9.20	5.65	5.35
ZnO	8.00	5.67	5.75
TiO ₂	6.00	5.77	5.83
SnO ₂	4.30	5.81	6.24
Cr ₂ O ₃	8.40	5.86	
α -Fe ₂ O ₃	8.60	5.92	
SiO ₂	2.00	6.19	6.46
WO ₃	0.43	6.64	6.53

amount of untreated powder in solution, the pH is stabilized; it corresponds to the PZZP. The electrochemical potential of the solution tend to align with the Fermi energy of the oxide (χ). Consequently, protonated species (or hydroxyl) are driven to the Helmholtz layer, leading to a pH change.

Therefore, as already suggested by Butler and Ginley [18], in a given electrolyte like water, the Fermi energy of the oxide, that is to say, electronegativity has to be connected to the PZZP. This correlation is shown in Fig. 6. An approximate function correlating the PZZP to pH can be deduced: $\chi_{\text{oxide}} = -0.09\text{PZZP} + 6.45$. The correlation proposed by Butler and Ginley is: $\chi_{\text{oxide}} = -0.12\text{PZZP} + 6.45$.

6. Surface reactivity of oxide nanoparticles

Nanoparticles prepared following the processes described in Fig. 1 have to be treated to be practically used. For example, maghemite nanoparticles, used in the development of magnetic synthetic carriers in blood circulation, precipitate at the physiological pH (7.35–7.45). They have to be coated generally with polymer; in this case, the stabilisation is due to a steric repulsion that prevents the coalescence of particles [20,21]. It is also possible to coat the nanoparticles stabilized by electrostatic repulsion with organic molecules such as citrates, tartrates, and glutamates; in order to enlarge the pH domain of stability within, they remain in suspension [22]. For some in vivo biological applications, it is necessary

to form covalent bonding between the oxide and the molecule to prevent depletion of the polymer to the surface and a surface modification with organo-functionalized silane, before the coating of the polymer is suggested. The modification is generally done at room temperature via spontaneous reaction.

A simplified schematisation is shown in Fig. 7. If the electronegativities of the molecule and of the oxide are located at comparable energy, and if $2\eta'$ of the molecule is much smaller than 2η of the oxide or if $2\eta'$ is much larger than 2η , no spontaneous reaction can occur (Fig. 7b and c). On the contrary, if χ and χ' are very different and if η and η' have such values that HOMO and CB or LUMO and VB correspond to similar energies, then spontaneous reactions can occur (Fig. 7a and d).

6.1. Reactivity of nanoparticles with water

In the scope of this approach, it is tempting to study the reactivity of water vs. oxide particles (Fig. 7). Inside the gap of H₂O itself, it seems consistent to attribute the energy level of LUMO to the H⁺/H₂O couple, which is located at 4.5 eV of the vacuum level [19]. Energy of HOMO is located 1.23 eV higher, i.e. at about 5.73 eV. One can deduce that the electronegativity of water, in between these two levels, is around 5.1 eV.

In a first approximation, neglecting the subband-gap levels, Fig. 7 shows that SiO₂, Al₂O₃ and α -Fe₂O₃ particles have to be stable in water. It corresponds to the case (d): electronegativity values of water and oxides are comparable and the water window is located inside the oxide gaps.

6.2. Surface modification by silanization

An original approach for the stabilization and functionalization of nanoparticles is surface modification by silanization. The coupling agents have a general formula: R-(CH₂)₃-Si-R', where R is an organic functional group (-NH₂, -NH-(CH₂)₂-NH₂, -SH, ...) and R' an alkoxy group [23].

Let us examine the case of the surface modification of maghemite nanoparticles by the γ amino-

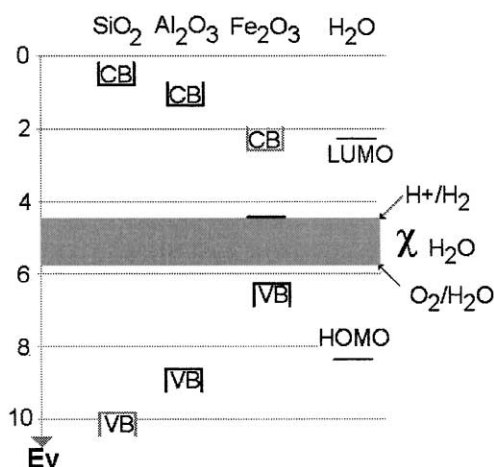
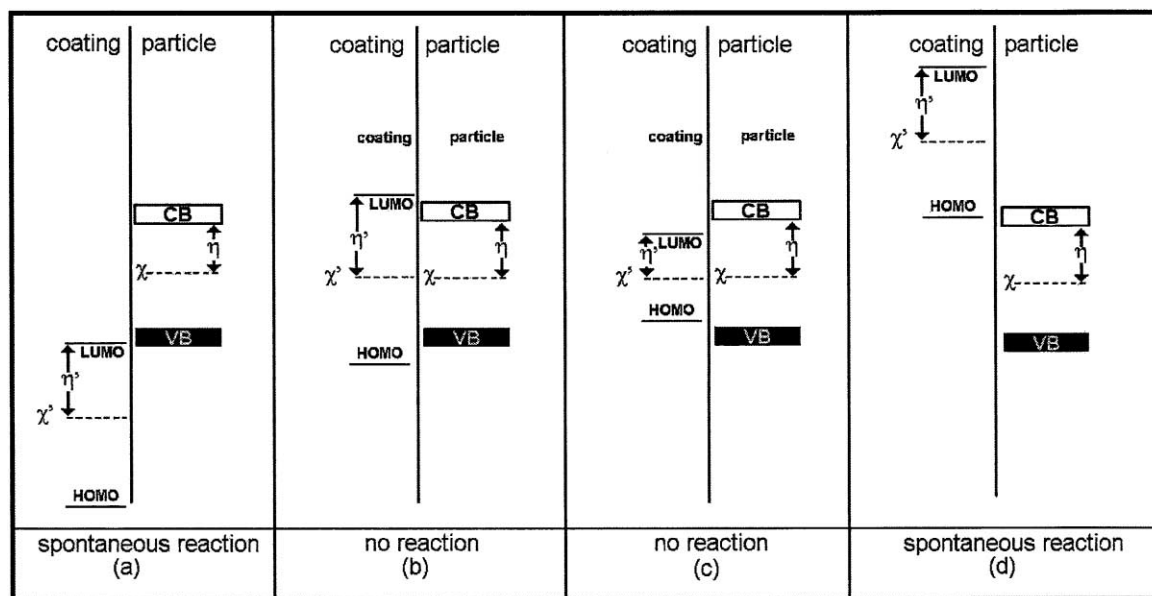


Fig. 7. Upper diagram: schematic representation of the various energy levels for a reacting molecule (HOMO, LUMO) and for the oxide to coat (valence band, VB and conduction band, CB). Lower diagram: application to water vs. SiO_2 , Al_2O_3 and $\alpha\text{-Fe}_2\text{O}_3$.

propyltrimethoxysilane (γ APS). It is well known that an efficient coating is obtained in the case of silica or alumina particles. An excess of γ APS was added in an acidic maghemite sol (Fig. 8). The methoxysilane group's hydrolysis into silanol groups is catalysed by the acidic way and the presence of amino groups allows to catalyse the condensation by the basic way. There is no doubt about the formation

of the Fe–O–Si bond [24]. However, Xu et al. [25] have considered that amino groups could be bound onto the maghemite surface. Two spontaneous reactions can in fact occur: (i) silanization of the particle with formation of a covalent –Fe–O–Si bond, and (ii) formation of bond between the amino group and iron in the particle (complexation). This behaviour seems to show that reactions (i) and (ii) occur simul-

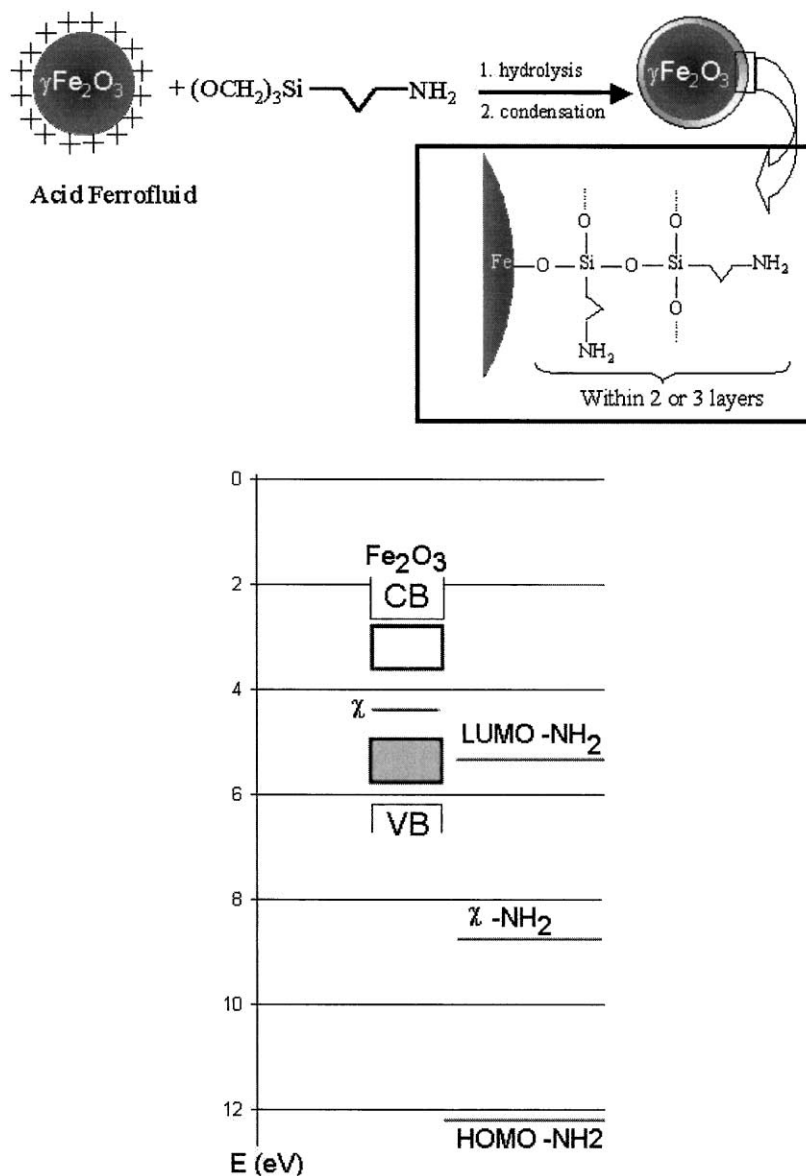


Fig. 8. Surface modification of maghemite nanoparticles by γ APS in aqueous medium and comparison of energy levels in Fe_2O_3 and in $-\text{NH}_2$ group. The data for $-\text{NH}_2$ group are from Ref. [26].

taneously. LUMO orbitals and valence band of Fe_2O_3 are actually located at a comparable energy (Fig. 8).

7. Conclusion

Electronegativity, χ , and chemical hardness, η , are used as fundamental tools for the preparation of

oxide nanoparticles and for the interpretation of their physical and chemical properties. The electronegativity is unchanged from crystal to nanoparticles when the chemical hardness diminishes. χ, η plot permits to forecast the type of nanoparticle formed in inorganic salt solutions. A linear relation is obtained between PZZP and pH. A model approach concern-

ing the surface modification of oxide nanoparticles by silanization is proposed.

Acknowledgements

The authors are indebted to Antoine Villesuzanne and Jean-Pierre Doumerc for helpful discussions and to DuPont de Nemours for financial support.

References

- [1] L. Pauling, *J. Am. Chem. Soc.* 54 (1932) 3570.
- [2] R.S. Mulliken, *J. Chem. Phys.* 2 (1934) 782.
- [3] R.G. Pearson, *J. Am. Chem. Soc.* 85 (1963) 3533.
- [4] R.G. Pearson, *J. Chem. Educ.* 45 (9) (1968) 581.
- [5] R.G. Pearson, *J. Chem. Educ.* 2 (76) (1999) 267.
- [6] R.G. Parr, R.G. Pearson, *J. Am. Chem. Soc.* 105 (1983) 7512.
- [7] J. Portier, G. Campet, *J. Korean Chem. Soc.* 41 (8) (1997) 437.
- [8] J. Portier, G. Campet, C.W. Kwon, A. Poquet, J. Etourneau, *Int. J. Inorg. Mater.*, accepted.
- [9] χ and η data can be found at: <http://www.icmcb.u-bordeaux.fr/pub/elecprop/ions.htm>.
- [10] M.H. Brodsky (Ed.), *Topics in Applied Physics Amorphous Semiconductors*. 2nd edn., Springer-Verlag, 1985.
- [11] G. Campet, S.J. Wen, S.D. Han, M.C.R. Shastry, J. Portier, *Mater. Sci. Eng. B* 18 (1993) 201.
- [12] G. Campet, C. Geoffroy, J.P. Manaud, J. Portier, Z.W. Sun, J. Salardenne, P. Keou, *Mater. Sci. Eng. B* 8 (1991) 45.
- [13] S.D. Han, N. Treuil, G. Campet, J. Portier, C. Delmas, J.C. Lassègues, A. Pierre, *Mater. Sci. Forum* 152 (1994) 217.
- [14] N. Treuil, C. Labrugère, M. Menetrier, J. Portier, G. Campet, A. Deshayes, J.C. Frison, S.J. Hwang, S.W. Song, J.H. Choy, *J. Phys. Chem. B* 103 (1999) 2100.
- [15] J.H. Choy, Y.I. Kim, B.W. Kim, G. Campet, J. Portier, P.W. Huang, *J. Solid State Chem.* 142 (1999) 368.
- [16] P. Poizot, S. Laruelle, S. Grugeon, L. Dupont, J.M. Tarascon, *Nature* 407 (2000) 496.
- [17] M. Henry, J.P. Jolivet, J. Livage, *Struct. Bonding* 77 (1992) 153.
- [18] M.A. Butler, D.S. Ginley, *J. Electrochem. Soc.* 125 (2) (1978) 228.
- [19] S.R. Morrison, *Electrochemistry at Semiconductor and Oxidized Metal Electrodes*. Plenum, 1980.
- [20] R. Evans, D.H. Napper, *Kolloid-Z. Z. Polym.* 251 (1973) 409.
- [21] R. Evans, D.H. Napper, *Kolloid-Z. Z. Polym.* 251 (1973) 329.
- [22] N. Fauconnier, Paris VI Thesis, 1996.
- [23] E.P. Plueddmann, *Silane Coupling Agents*. 2nd edn., Plenum, 1991.
- [24] M. Klotz, A. Ayral, C. Guizard, C. Ménager, V. Cabuil, *J. Colloid Interface Sci.* 220 (2) (1999) 357.
- [25] Z. Xu, Q. Liu, J.A. Finch, *Appl. Surf. Sci.* 120 (1997) 269.
- [26] D. Bergmann, J. Hinze, *Struct. Bonding* 66 (1987) 145.